International Journal of Engineering Research & Technology (IJERT)
ISSN: 2278-0181
Vol. 2 Issue 4, April - 2013

# Performance Analysis In Various Data Rate And Channel Model Of IEEE 802.15.3a System Based On UWB Communications.

Hashibul Alam
M-tech, Electronics and Communication Engineering Department, Narula Institute of Technology, WBUT, India.

Dola B. Gupta
Assistant Professor, Electronics and Communication Engineering Department, Narula Institute of Technology, WBUT, India.

P. K. Banerjee
Retired Prof. , Jadavpur University, Kolkata, India.

***Abstract-*** *In this paper detail analysis of modified S-V modelling of IEEE 802.15.3a standard UWB propagation channel is done and implemented for simulation of the UWB channel model in MATLAB. The simulation results of four different environments are obtained. A practical system is designed using MB-OFDM technology for Ultra–wideband communication to transmit high-speed data in an indoor environment. Lastly, BER performance analysis of the system model for various channels in SV channel model and various data rates are compared.*



## 1. Introduction

Ultra-wideband (UWB) has emerged as an stimulating technology for short range, very high data rate, based on short rang (nanosecond scale) waveforms for wireless communications. In 2002, the Federal Communications Commission (FCC) agreed on the allocation of a 3.1–10.6 GHz spectrum for unlicensed use of UWB devices [1]. In 2002, the FCC also define that any signal having a −10 dB fractional bandwidth larger than 20 %, or a signal bandwidth greater than 500 MHz is consider as UWB. The IEEE 802.15.3a wireless personal area networks (WPAN) standardization group proposed a very high data rate (up to 480Mbps) physical layer based on UWB. These systems used extremely low transmit power (an EIRP of -41.3 dBm/MHz) avoid the interference specified by FCC. The channel designing is very important for wireless communication. For wireless communication main problem arises due to multi-path. So a model was needed that could give true reflection of propagation characteristics of UWB signal under the multi-path environment. This is taken care of in modified Salen-Valenzula (S-V) model [2]. The MB-OFDM approach divides UWB spectrum (3.1–10.6 GHz) to multiple non-overlapping bands and for each band, transmission is done with OFDM.

## 2. System Model

The system consists of various system blocks as shown in **figure 1**. The system model begins with a Bernoulli binary generator, it is generates a frame-based random binary numbers using Bernoulli distribution. The Bernoulli Binary Generator is followed by a Channel Encoder. The channel encoding technique used is forward error correction code like Convolution coding and puncturing. Puncturing is a very effective and powerful adaptive coding technique; it removes some parity bits at transmitter and increases the coding rate. Succeeding it is a bit Interleaver which provides robustness against burst error and narrow-band interferers. The signal output of interleaver is modulated using QPSK, a multicarrier modulation technique, which gives high spectral efficiency. Robustness against transmission employs a frequency hopping technique in which the band is hopped using a time-frequency code (TFC) known to both transmitter and receiver. The transmission of OFDM symbols are done in more than one frequency sub-bands shown in figure 2. This results in frequency diversity and improves the performance in the presence of other non-coordinated devices. In this model the UWB MB-OFDM model which employs the first three sub-bands of 528 MHz (from 3.1 GHz to 4.7 GHz). After that, the signal propagates through the UWB channel. Cyclic prefix is use to reduce ISI and ICI introduced by the multi-path OFDM signal propagation. But in case of MB-OFDM system zero padding prefix (ZPP) is used. The advantage of using a ZPP is that the power back off at the transmitter can be avoid and less ripples are found in power spectral density [4]. In this system Viterbi decoder is used for decoding transmitting data in MB-OFDM system. The Viterbi Decoding [5], [6] Algorithm is used to find the stream of data that is sent among all possible streams. Ultimately, the path that accumulated the least amount of errors was chosen for transmission.

Hence it can be justified that this system gives high transmission speed due to multi-band OFDM, great system storage, excellent multipath immunity capacity, limited power wastage for usage of ZPP and low cost. So this technology is considered as a key technology to next generation indoor wireless communication.

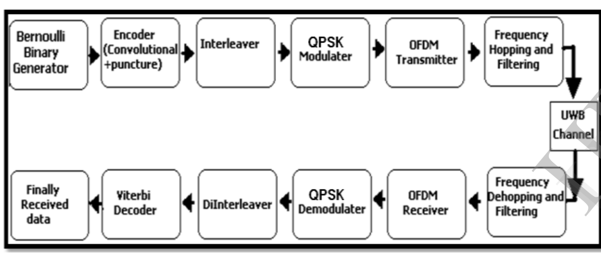


**Figure 1:** The block diagram of IEEE802.15.3a (WPAN) MB-OFDM system.

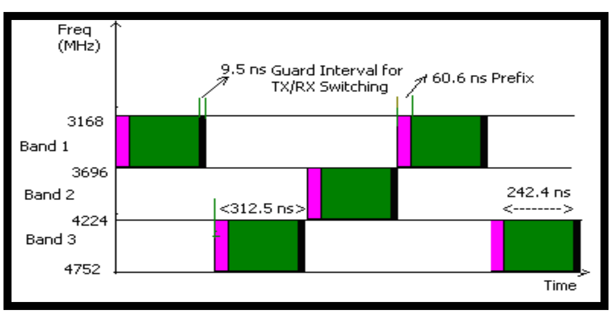


**Figure 2:** Example of time-frequency coding for the multiband OFDM system.

## 3. Channel Model

The channel model used for simulation is the one adopted by the IEEE 802.15.3a committee for the evaluation of UWB physical layer proposals [3]. It is a modified version of the Saleh-Valenzuela model for indoor channels, fitting the properties of measured UWB channels. A lognormal distribution is used mining the multi path gain magnitude.

Initially the Channel models were Poisson model [7]. In indoor communication, it is assumed that there is only one cluster of multipath in impulse response and the arrived multipath components are also considered as Poisson process.

The modified Poisson model was introduced which can describe the important multipath forepart arrived components better in line-of-sight (LOS) channels. At LOS conditions, the amplitude of the forepart arrived multipath is bigger than the latter's.

The Δ-K model [8] is improvement over standard Poisson model. This model provides the describing methods of the clustering of the multipath arrivals in UWB channel. It could not best fit the measurement data of indoor UWB channel in many cases.

The best suited model is the Saleh-Valenzuela model (S-V) [9]. This model describes the multipath arriving in clusters. That is the universal statistic model of indoor dispersion channel; in most of the cases this best fit the statistics of the measured data. However it has some demerits which are: it can exact reflect the propagation law of indoor NLOS environment, it can not give exact reflect the propagation law of indoor LOS environment and this model also cannot give exact prognosticate the multipath propagation characteristics of given indoor condition.

Then the IEEE workgroup made some modification on the S-V model. Where they used log-normal distribution to express multipath plus amplitude, and using another log-normal stochastic variable to express general multipath plus fluctuation. The impulse response of modified Saleh-Valenzuela model expressed as (1).

$$h_i(t) = X_i \sum_{l=0}^{L-1} \sum_{n=0}^{N-1} \alpha_{n,l}^{i} \, \delta(t - T_l^{i} - \tau_{n,l}^{i}) \quad (1)$$

Where $\alpha_{n,l}^{i}$ are the multipath gain coefficients, $T_{n,l}^{i}$ represents the delay of the $l^{th}$ cluster, $\tau_{n,l}^{i}$ is the delay of the $n^{th}$ multipath component relative to the $l^{th}$ cluster arrival time $T_l^i$, $X_i$ represents the log-normal shadowing and i represents the $I^{th}$ realization.

Saleh-Valenzuela model can not assume the arrival of paths in each sampling interval time. However, the two Poisson models are use to modeling the arrival interval [10]. The arrival times of each cluster as well as rays in each cluster follow an individual Poisson process shown in **figure 3**. The Poisson distribution of cluster arrival time and the ray arrival time can be expressed as (2) and (3) [11].

$$P(T_l / T_{l-1}) = \Lambda \exp[-\Lambda(T_l - T_{l-1})],\ l > 0 \qquad (2)$$

$$P(\tau_{n,l} / \tau_{(n-1),l}) = \lambda \exp[-\lambda(\tau_{n,l} - \tau_{(n-1),l})],\ n>0,\ l>0 \qquad (3)$$

Where Λ is the cluster arrival rate, λ represents ray arrival rate, **Γ** is represents cluster decay factor and γ is represents ray decay factor.

So finely, new modified Saleh-Valenzuela model impulse response expressed as (4), which correlated with the time-of-arrival and angle-of-arrival.

$$h(t,\theta) = \sum_{l=0}^{L-1}\sum_{n=0}^{N-1} \beta_{n,l}\, e^{i\theta_{n,l}}\, \delta(t - T_l^i - \tau_{n,l}) \qquad (4)$$

Where, $\beta_{n,l}$ is statistically independent positive random variable and $\theta_{n,l}$ is statistically independent uniform random variable.

Commonly, it is correlated with the arrival time and arrival angle. If the arrival time and arrival angle of multipath components have depended, then the excursion of the cluster mean square angle will lead to longer delay. However, from the measurements of Spencer and Rice, it was showed that the channel characteristics dissatisfied this point [12]. Due to the independency of the time and angle completeness impulse response sequence written as

$$h(t,\theta) = h(t)h(\theta) \qquad (5)$$

in this way, $h(\theta)$ is absolutely independency. Based on the S-V model, the new $h(t)$can be written as

$$h(t) = \sum_{l=0}^{L-1}\sum_{n=0}^{N-1} \beta_{n,l}\, \delta(t - T_l^i - \tau_{n,l}) \qquad (6)$$

$h(\theta)$ is an independence angle impulse response, it can be considered as a model which is similar to the channel time impulse response, and the model is given by

$$h(\theta) = \sum_{l=0}^{L-1}\sum_{n=0}^{N-1} \delta(\theta - \omega_{n,l}) \qquad (7)$$

Where $\omega_{n,l}$ is the arrival angle of the $n^{th}$ path within the $l^{th}$ cluster.

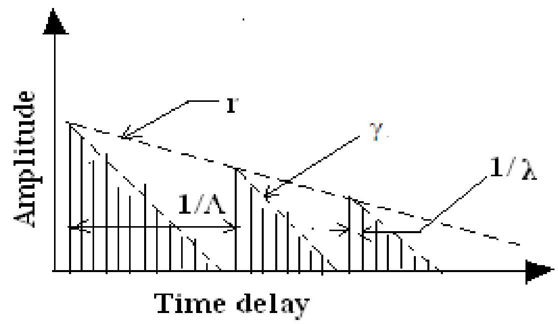


**Figure 3:** Saleh-Valenzuela (S-V) model.

### 3.1 Channel Parameters

The following T**able 1** lists Saleh-Valenzuela model parameters for four different channel model characterizations from measurement data by Intel [13].

In our simulations, we have used the UWB channel models CM1 to CM4 specified in the IEEE802.15.3a channel modeling sub-committee report [3].

- **CM1:-** This channel model based on LOS (0 – 4 m) channel.
- **CM2:-** This channel model based on NLOS (0 – 4 m) channel.
- **CM3:-** This channel model based on NLOS (4 – 10 m) channel
- **CM4:-** This channel model based on NLOS (4 – 10 m)

**Table 1:** IEEE802.15.3a Channel Parameters.

| **Model Parameters** | **CM1** | **CM 2** | **CM 3** | **CM 4** |
|---|---|---|---|---|
| Cluster arrival rate Λ (1/nsec) | 0.0233 | 0.4 | 0.0667 | 0.0667 |
| Ray arrival rate λ (1/nsec) | 2.5 | 0.5 | 2.1 | 2.1 |
| Cluster decay factor Γ | 7.1 | 5.5 | 14 | 24 |
| Ray decay factor γ | 4.3 | 6.7 | 7.9 | 12 |
| standard deviation of cluster lognormal fading σ1 (dB) | 3.394 | 3.394 | 3.394 | 3.394 |
| standard deviation of ray lognormal fading σ2 (dB) | 3.394 | 3.394 | 3.394 | 3.394 |

| | | | | |
|---|---|---|---|---|
| standard deviation of lognormal shadowing term for total multipath realization σx (dB) | 3 | 3 | 3 | 3 |
| **Model Characteristics** | | | | |
| Mean excess delay (ns) ($\tau_m$ ) | 5 | 9.9 | 15.9 | 30.1 |
| RMS delay (ns) ($\tau_{rms}$) | 5 | 8 | 15 | 25 |
| NP (85%) | 20.8 | 33.9 | 64.7 | 123.3 |
| NP10dB | 12.5 | 15.3 | 24.9 | 41.2 |
| Channel energy mean (dB) | -0.4 | -0.5 | 0 | 0.3 |
| Channel energy std (dB) | 2.9 | 3.1 | 3.1 | 2.7 |

## 4. Simulation Results

In this subsection, the authors present simulation results in order to compare and analyze the performance of the receiver described in different indoor UWB channel scenarios defined in [3]. An extensive study on IEEE 802.15.3a have been done by changing the data rates for five different values (240,200,160,110,106.6) Mbps compared to standard reference data rate of 200 Mbps and keep same spreading rate 2. In the simulations, the UWB channel models CM1 to CM4 specified in the IEEE802.15.3a channel modeling sub-committee report is used [3].

Firstly, the channel models are analysed based on the Saleh-Valenzuela model [2], where multipath components arrive in clusters. The Discrete-time impulse responses of the four different modified S-V models are shown in **Figure 4**. Where it is seen that paths in CM1 tend to concentrate in two clusters with smaller delay and CM2 tend to concentrate in three clusters with delay more then CM1 and CM3 tend to concentrate in four or five clusters with delay more then CM2 and CM4 paths tend to spread over more clusters with higher delay.

.



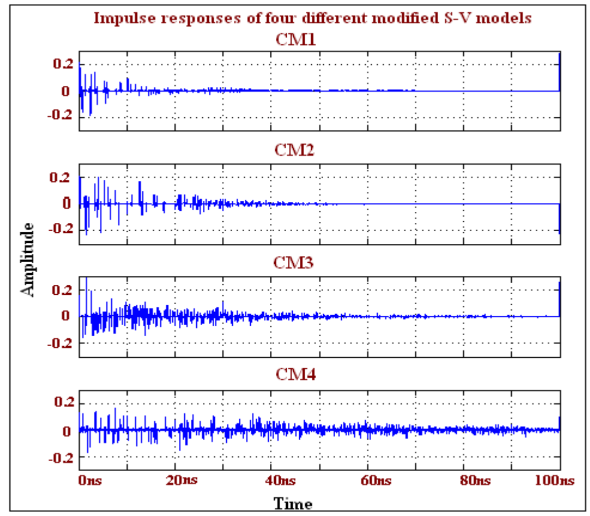


**Figure 4:** Delay profiles for Modified Saleh-Valenzuela channel CM1 to CM4.

Secondly, we have analyzed the system by changing the channel model keeping the data rate fixed at 240 Mbps. The obtained graphs for constellation diagram and the corresponding PSD are given. The received signal constellations after channel estimation and synchronization are shown in **Figure (5 to 8)**.

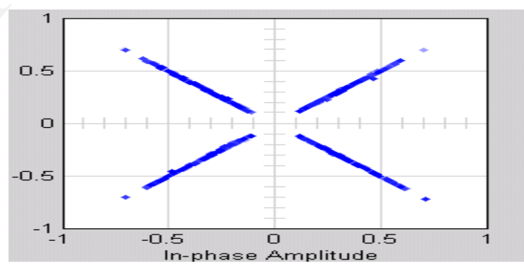


**Figure 5:** Signal constellations diagram after channel estimation and synchronization for CM1.

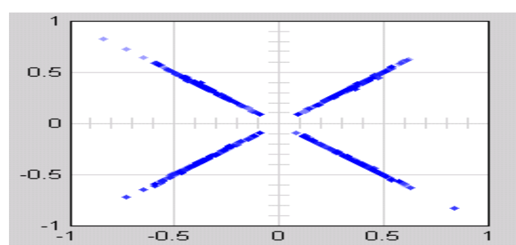


**Figure 6:** Signal constellations diagram after channel estimation and synchronization for CM2.

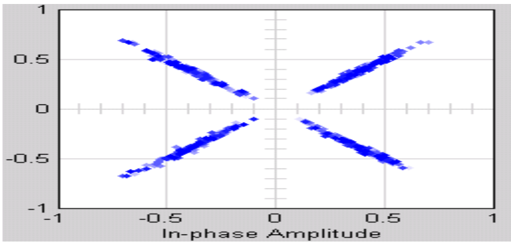


**Figure 7:** Signal constellations diagram after channel estimation and synchronization for CM3.

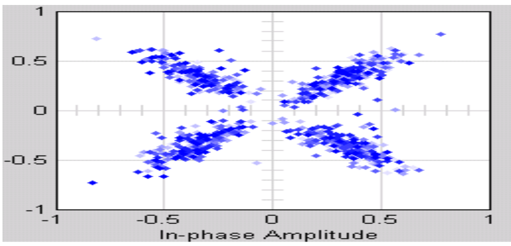


**Figure 8:** Signal constellations diagram after channel estimation and synchronization for CM4.

It is seen that the constellation diagram more spread when the channel models are changed from 1 to 4 and distributed X-shaped due to increasing delay. The received signals PSD are shown in **Figure (9 to 12)**. It is seen that the PSD is more rippled when the channel models are changed from 1 to 4.

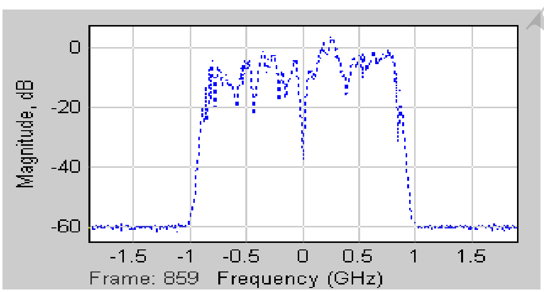


**Figure 9:** PSD diagram at 240 Mbps for CM1.

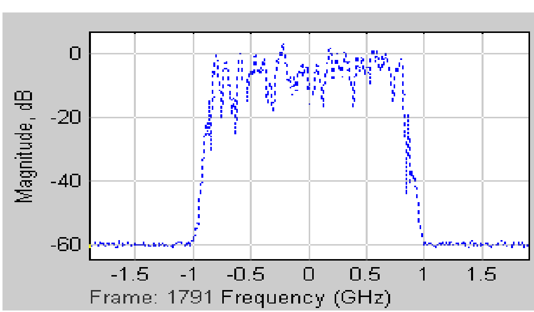


**Figure 10:** PSD diagram at 240 Mbps for CM2.

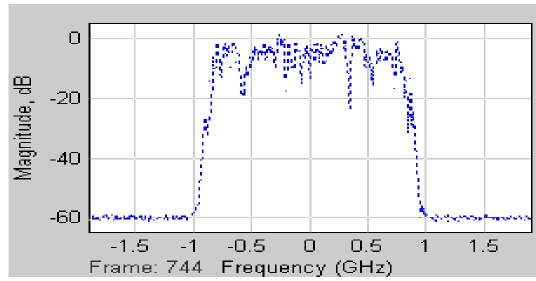


**Figure 11:** PSD diagram at 240 Mbps for CM3.

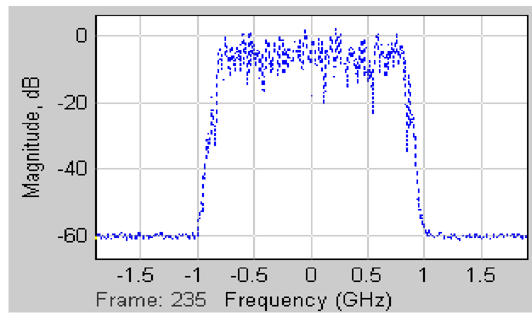


**Figure 12:** PSD diagram at 240 Mbps for CM4.



Thirdly, for different code rates (1/3, 11/32, ½, 5/8, 3/4) and keeping the channel model same (CM1) the system model the PSD are shown **Figure (13 to 17)**. The PSD obtained clearly shows that the spectrum non overlapping for the code rates 1/3 and 11/32 and spectrum overlapping for code rates ½, 5/8 and 3/4. This is due to fact that, due increase code rate, effective bandwidth increases and as a results increases data rates (106.6 110,160, 200,240) Mbps.

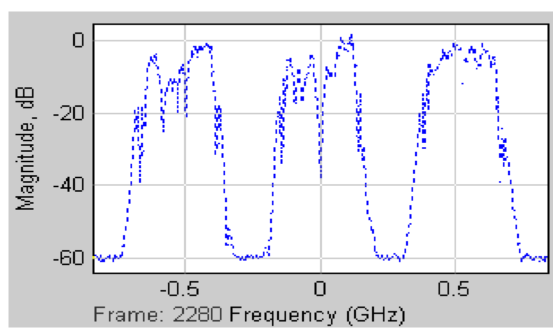


**Figure 13:** PSD diagram for 106.6 Mbps data rate.

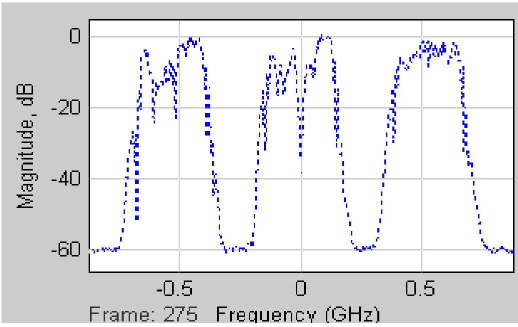


**Figure 14:** PSD diagram for 110 Mbps data rate.

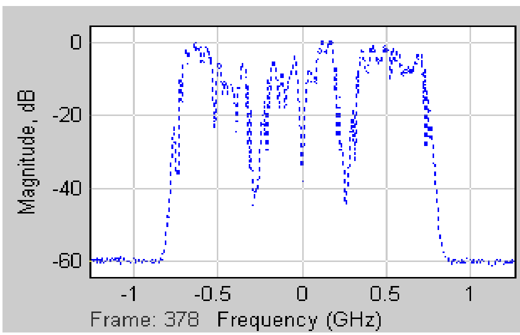


**Figure 15:** PSD diagram for 160 Mbps data rate.

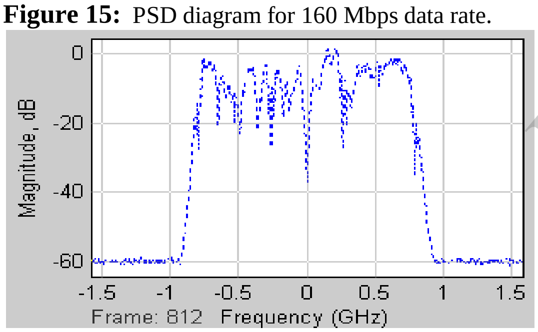


**Figure 16:** PSD diagram for 200 Mbps data rate.

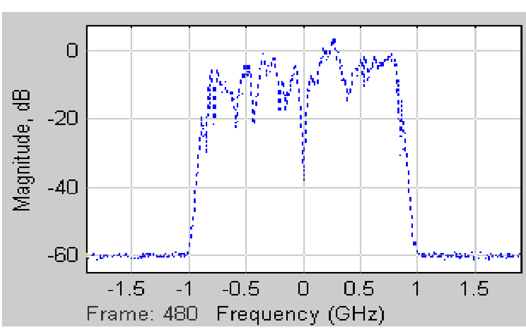


**Figure 17:** PSD diagram for 240 Mbps data rate.

Fourthly, we have analysis the BER performance of the MB-OFDM system, over the different channel model (CM1 to CM4), taken set of data rates 106.6, 110, 160, 200 and 240 Mbps. The obtained graphs are shown in **Figure (18 to 21)** and $E_b/N_0$ (dB) value at $10^{-3}$ BER for each data rate and channel model can be seen tabular form in Table 2.

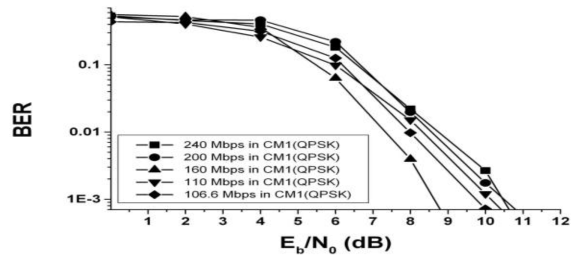


**Figure 18:** BER performance at various data rates of the MB-OFDM system for CM1.



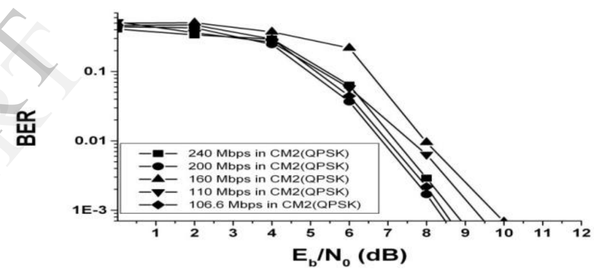


**Figure 19:** BER performance at various data rates of the MB-OFDM system for CM2

.

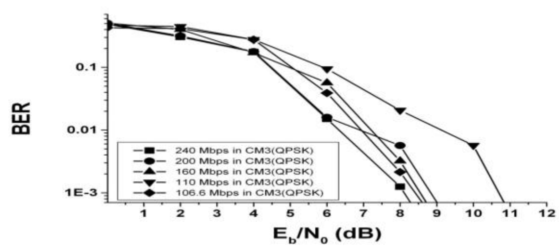


**Figure 20:** BER performance at various data rates of the MB-OFDM system for CM3

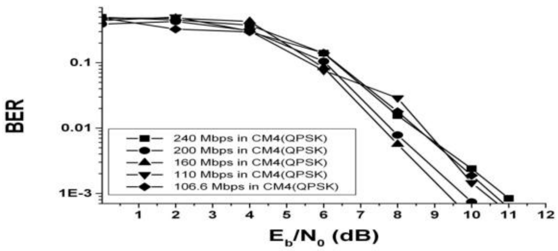


**Figure 21:** BER performance at various data rates of the MB-OFDM system for CM4.

Then we have also analysis same think, over the different data rates (240, 200, 160, 110 and 106.6 Mbps.), taken channel model CM1, CM2, CM3 and CM4 are shown in **Figure (22 to 26)**.

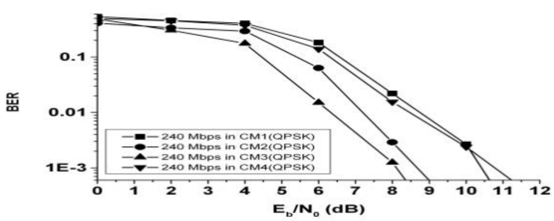


**Figure 22:** BER performance for various channel models at fixed data rate 240 Mbps.

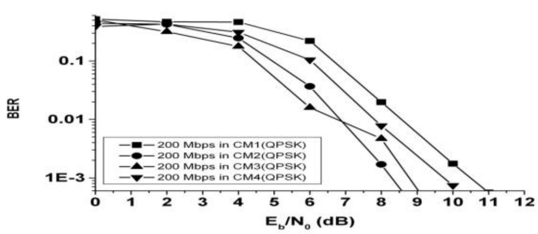


**Figure 23:** BER performance for various channel models at fixed data rate 200 Mbps.

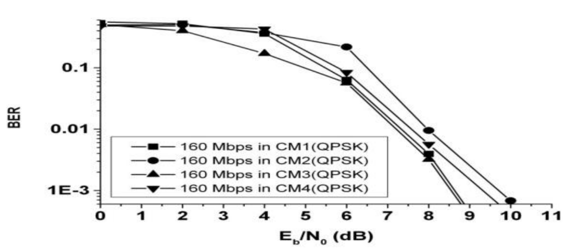


**Figure 24:** BER performance for various channel models at fixed data rate 160 Mbps.

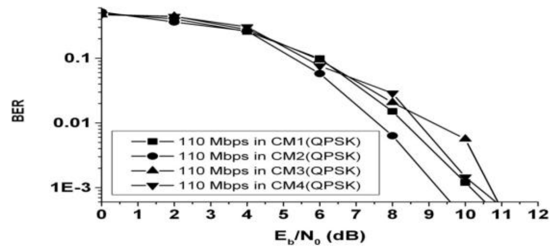


**Figure 25:** BER performance for various channel models at fixed data rate 110 Mbps.

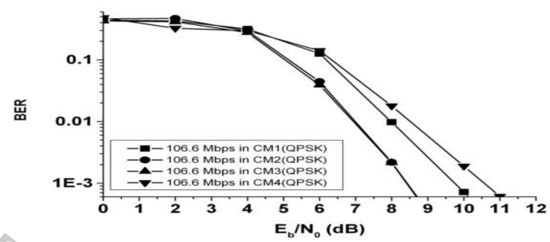


**Figure 26:** BER performance for various channel models at fixed data rate 106.6 Mbps.



**Table 2:** BER performance of MB-OFDM system for various channel models and data rates.

| Channel model (CM) | Data rates (Mbps) | BER | $E_b/N_0$ (dB) |
|---|---|---|---|
| CM1 | 240 | $10^{-3}$ | 10.6 |
| | 200 | $10^{-3}$ | 10.8 |
| | 160 | $10^{-3}$ | 8.8 |
| | 110 | $10^{-3}$ | 10.4 |
| | 106.6 | $10^{-3}$ | 10 |
| CM2 | 240 | $10^{-3}$ | 8.9 |
| | 200 | $10^{-3}$ | 8.5 |
| | 160 | $10^{-3}$ | 10 |
| | 110 | $10^{-3}$ | 9.5 |
| | 106.6 | $10^{-3}$ | 8.6 |
| CM3 | 240 | $10^{-3}$ | 8.25 |
| | 200 | $10^{-3}$ | 9 |
| | 160 | $10^{-3}$ | 8.7 |
| | 110 | $10^{-3}$ | 10.8 |
| | 106.6 | $10^{-3}$ | 8.6 |
| CM4 | 240 | $10^{-3}$ | 11.15 |
| | 200 | $10^{-3}$ | 10 |
| | 160 | $10^{-3}$ | 9.55 |
| | 110 | $10^{-3}$ | 10.65 |
| | 106.6 | $10^{-3}$ | 10.8 |

## 5. Conclusion

In this paper, the analysis is done based on simulation of statistical model for the propagation of UWB signals ,in various indoor environments for both LOS and NLOS scenarios. The delay profile figures from MATLAB illustrate the impulse response of the modified S-V channel model. Where it can be seen that the increase in code rate increases the bandwidth as a result data rate increases which is depicted from PSD Diagram. The BER vs. Eb/No plots show the performance of the MB-OFDM system. In this simulation, it is shown that the system can be affected by multi-path fading but this system has high anti-noise ability low BER and wide coverage.

The channel models based on the Saleh-Valenzuela model [2], where multipath components arrive in clusters are analysed. The Discrete-time impulse responses of the four different modified S-V models are shown in Figure 4. The signal constellation plot reveals that the density of the plot increases as the channel model varies from CM1 to CM4 for all data rates. The corresponding PSD plot is also shown. The system is simulated for all the four channels with various data rates with QPSK modulation. The BER analysis of the whole system is done.



## References

[1] "First report and order, revision of part 15 of the commission's rules regarding ultra-wideband transmission systems," FCC, ET Docket 98-153, Feb. 14, 2002.
[2] A. Saleh and A. Valenzuela, "A statistical model for indoor multipath propagation," *IEEE J. Selected Areas in Commun.*, pp. 128–137, February 1987.
[3] J. Foerster, "Channel modeling sub-committee report final," Tech. Rep., IEEE802.15-02/490, 2003.
[4] Anuj Batra, Jaiganesh Balakrishnan, and Anand Dabak "Multi-band ofdm: a new approach for UWB" 0-7803-8251-X/04, IEEE 2004.
[5] G. D. Forney, "The Viterbi algorithm," *Proceedings of the IEEE*, vol. 61, no. 3, pp. 268–278, March 1973.
[6] B. Vucetic and J. Yuan, *Turbo Codes Principle and Applications*, Kluwer Academic Publishers, 2000.
[7]Theodore S. Rappaport, "Wireless Communicationd", Prentice-Hall of India, 2007.
[8] B. Kannan et al, "UWB Channel Charactrization in office environments" IEEE Tech. Rep. Document, IEEE802.15-04-0439-00-004a, 2004.
[9] Molish A F. Ultra-wideband propagation channels theory, measurement and modeling [J]. IEEETrans.Veh.Technol, 2005, 54 (5):1528-1545.
[10] J.R.Foerster.Channel modeling sub-committee report final [J].IEEE P802.15-02/368r3-SG3a Sep.4, 2002.
[11] J. R. Foerster, M. Pendergrass, and A. F. Molisch, "A UWB channel model for ultrawideband indoor communication", Proc. WPMC 2003, (2003).
[12] Quentin Spencer, Michael Rice, Brian Jeffs and Michael Jensen "Indoor Wideband Time/Angle of Arrival multipath propagation Results" IEEE o-7803-3659-3/97, pp. 1410-1414, 1997.
[13] J. Foerster, "Channel Modeling Sub-committee Report," IEEE P802.15-02/368r1-SG3a. November 5, 2002.